A MTL Transmission Matrix Method for Transmission-Lines with Differential Setup

Licinius D. S. Alcantara, João C. W. Albuquerque Costa, Member, IEEE, Boris Dortschy and Aldebaro Klautau, Member, IEEE

***Abstract*—A transmission matrix approach extended to a multiconductor model is employed to analyze crosstalk interference over telephone lines. Simulations and analysis concerning a standard telephone loop topology are carried out to validate the proposed technique.**

***Index Terms*—MTL theory, transmission line modeling, digital subscriber line, ABCD matrix, last mile connectivity.**

I. Introduction

Crosstalk noise from similar digital services of physically adjacent loops is the primary impairment to send digital information through usual transmission lines, such as twisted-pair loops, which are nowadays used as inexpensive channels for last mile Internet access. Crosstalk is even more impacting as the operating frequency increases and can be more intense than the direct signal, being thus a concern for Internet providers based on Digital Subscriber Line (DSL) technology. Crosstalk to a receiver from a neighboring transmitter is called near-end crosstalk (NEXT), and crosstalk to a receiver from a transmitter at the opposite end is called far-end crosstalk (FEXT).

Previous crosstalk characterization efforts, such as model developments based on statistical data, were not satisfactory for use on multiple-input multiple-output (MIMO) transmission techniques. Therefore, new channel models have been proposed. In order to better understand and predict signal interference between neighboring pairs, the electromagnetic compatibility (EMC) community has been dispending efforts to achieve a physical model for cable binders, based on electric and magnetic parameters. For a long time, the EMC community has studied crosstalk and transmission properties of cable binder under differential excitation with various levels of approximations [1]-[3].

This work was supported by the Research and Development Centre, Ericsson Telecomunicações S.A., Brazil. L. D. Alcantara, J. Costa and A. Klautau are with the Federal University of Pará, Tucuruí/Belém, PA 66075-900, Brazil (phone: +55-91-8157-9862; fax:+55-91-3201-7634); e-mails: {licinius,jweyl,aldebaro}@ufpa.br. B. Dortschy is with the ASP Lab, Ericsson EAB, Kista, Sweden. E-mail: boris.dortschy@ericsson.com.

The circuit theory for a binder MIMO channel is based on multiconductor transmission line (MTL) theory [5], [5]. In MTL, a basic loop segment consists of two or more transmission lines coupled via distributed mutual capacitive, inductive and ohmic parameters. Similarly as occurs in the case of single line analysis, each basic MTL segment can also be mathematically expressed as a transmission matrix (or ABCD matrix), which is a frequency domain method. The main advantage of the transmission matrix approach is that the complete MTL cable loop can be treated as the cascade of many distinct serial MTL basic loop segments, if variations on the loop distributed parameters have to be modeled. In this case, the transmission matrix for whole loop is obtained from the product of the transmission matrixes of the loop segments with constant distributed parameters over the considered distance. Finally, essential information such as direct loop transfer functions and crosstalk transfer function can be retrieved from the resulting transmission matrix.

Differential setup means that sources and loads are individually applied to each pair of conductor wires, in contrast to common-mode setup, where one of the conductors is common to all pairs in a binder (the reference conductor). The differential setup is focused in this work because of its simpler practical implementation so that it is the chosen setup for telephone loops and other applications.

This work is organized as follows: In section II the differential equations for the MTL model are derived. Results for a standard telephone loop are shown in Section III. The final comments are presented in section IV.

II. MTL Model with Differential Setup

Fig. 1 shows the multiconductor basic segment [5], which is the reference for the mathematical derivations carried out on this section, where z denotes a position of the line, in meters. The parameters R_{ii}, L_{ij}, C_{ij} and G_{ij} are the distributed electric resistances (Ω/m), inductances (H/m), capacitances (F/m) and conductances (S/m), respectively. The signals V_i are the electric potentials (volts) and I_i are the electric currents (ampères). In this scheme, $V_1 = V_{1b} - V_{1a}$ and $V_2 = V_{2b} - V_{2a}$.

By applying the Kirchhoff current law on the uppermost conductor (“2b”), we obtain the following relation, valid for the second transmission-line (or second pair of conductors):

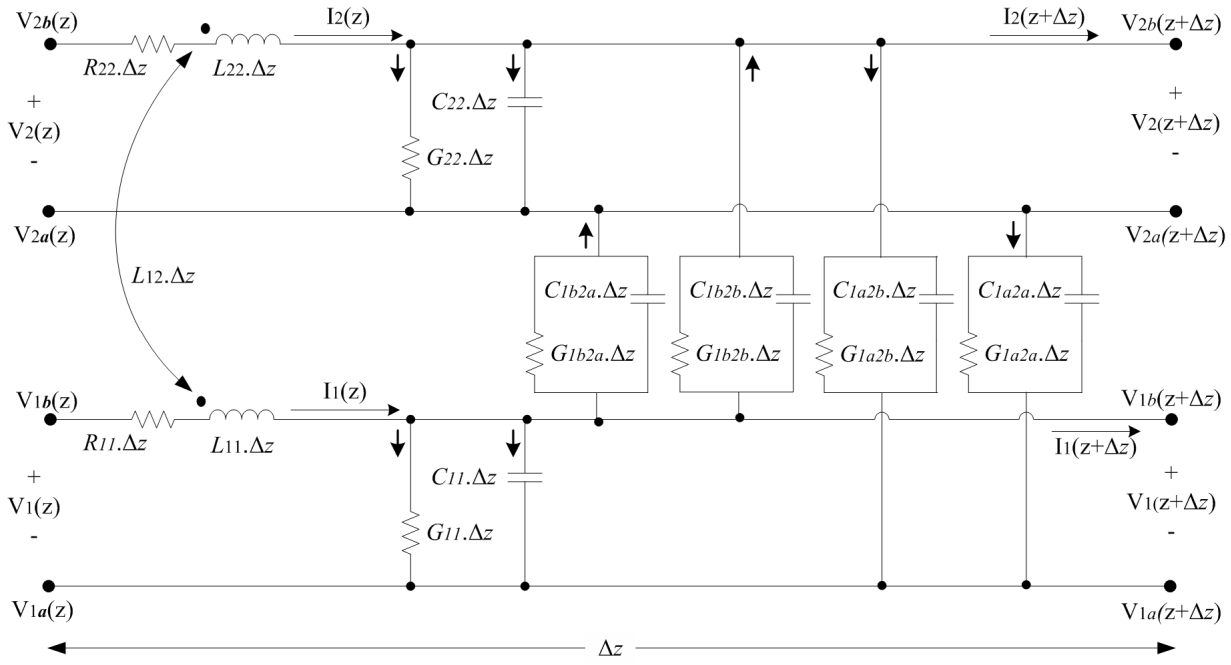

Fig. 1. The basic MTL segment adopted for two transmission line model with differential excitation.

$$
\begin{aligned}
&I_2(z) = I_2(z+\Delta z) + G_{22}\Delta z V_2(z+\Delta z) + \\
&C_{22}\Delta z \frac{\partial V_2(z+\Delta z)}{\partial t} - G_{1b2b}\Delta z\left[V_{2b}(z+\Delta z) - V_{1b}(z+\Delta z)\right] \\
&- C_{1b2b}\Delta z \frac{\partial}{\partial t}\left[V_{2b}(z+\Delta z) - V_{1b}(z+\Delta z)\right] \\
&+ G_{1a2b}\Delta z\left[V_{2b}(z+\Delta z) - V_{1a}(z+\Delta z)\right] \\
&+ C_{1a2b}\Delta z \frac{\partial}{\partial t}\left[V_{2b}(z+\Delta z) - V_{1a}(z+\Delta z)\right].
\end{aligned} \tag{1}
$$

The capacitance and conductance between different conductors depend on the distance and on the dielectric that apart them. Considering that the conductors of the same pair are very tight or twisted, the average distance between pairs can be considered to be approximately the same. Therefore, the following simplifications were considered for the mutual parameters:

$$
\begin{aligned}
&C_{1a2a} = C_{1a2b} = C_{1b2a} = C_{1b2b} = C_{12}, \\
&G_{1a2a} = G_{1a2b} = G_{1b2a} = G_{1b2b} = G_{12}.
\end{aligned} \tag{2}
$$

By considering (2) and taking the limit when $\Delta z \to 0$, then (1) is reduced to

$$
\begin{aligned}
&G_{22}V_2(z,t) + C_{22}\frac{\partial V_2(z,t)}{\partial t} \\
&+ G_{12}V_1(z,t) + C_{12}\frac{\partial V_1(z,t)}{\partial t} = -\frac{\partial I_2(z,t)}{\partial z}.
\end{aligned} \tag{3}
$$

In the same way, by applying the Kirchhoff current law on the third conductor ("1b"), we obtain the following relation for the first transmission-line:

$$
\begin{aligned}
&G_{11}V_1(z,t) + C_{11}\frac{\partial V_1(z,t)}{\partial t} \\
&- G_{12}V_2(z,t) - C_{12}\frac{\partial V_2(z,t)}{\partial t} = -\frac{\partial I_1(z.t)}{\partial z}.
\end{aligned} \tag{4}
$$

Now applying the Kirchhoff voltage law, for the first and the second transmission line, respectively, we obtain:

$$
R_{11}I_1(z,t) + L_{11}\frac{\partial I_1(z,t)}{\partial t} - L_{12}\frac{\partial I_2(z,t)}{\partial t} = -\frac{\partial V_1(z,t)}{\partial z}, \tag{5}
$$

$$
R_{22}I_2(z,t) + L_{12}\frac{\partial I_1(z,t)}{\partial t} + L_{22}\frac{\partial I_2(z,t)}{\partial t} = -\frac{\partial V_2(z,t)}{\partial z}. \tag{6}
$$

By considering a harmonic time-dependence *exp*(jωt), (4) and (3) can be rewritten respectively as:

$$
-\frac{\partial \mathrm{I}_1(z)}{\partial z} = Y_{11}V_1(z) - Y_{12}V_2(z) \tag{7}
$$

$$
-\frac{\partial \mathrm{I}_2(z)}{\partial z} = Y_{12}V_1(z) + Y_{22}V_2(z), \tag{8}
$$

where $Y_{ij} = G_{ij} + j\omega C_{ij}$ (*ij* =11, 22 or 12).

Rewriting the above equations in matrix form, we obtain:

$$
-\frac{\partial}{\partial z}\bar{\mathbf{I}} = \overline{\overline{\mathbf{Y}}}\,\overline{\mathbf{V}}, \tag{9}
$$

where $\bar{\mathbf{I}} = \left[I_1(z) \quad I_2(z)\right]^T$, $\overline{\mathbf{V}} = \left[V_1(z) \quad V_2(z)\right]^T$ and

$$
\overline{\overline{\mathbf{Y}}} = \begin{bmatrix} Y_{11} & -Y_{12} \\ Y_{12} & Y_{22} \end{bmatrix} = \begin{bmatrix} G_{11} + j\omega C_1 & -\left(G_{12} + j\omega C_{12}\right) \\ G_{12} + j\omega C_{12} & G_{22} + j\omega C_2 \end{bmatrix}, \tag{10}
$$

or

$$\overline{\overline{\mathbf{Y}}} = \overline{\overline{\mathbf{G}}} + j\omega\overline{\overline{\mathbf{C}}}\,, \tag{11}$$

where the distributed conductance and distributed capacitance matrices are given by

$$\overline{\overline{\mathbf{G}}} = \begin{bmatrix} G_{11} & -G_{12} \\ G_{12} & G_{22} \end{bmatrix} \text{ and } \overline{\overline{\mathbf{C}}} = \begin{bmatrix} C_{11} & -C_{12} \\ C_{12} & C_{22} \end{bmatrix}. \tag{12}$$

Now considering the harmonic time-dependence exp(jωt) for (5) and (6), we obtain:

$$-\frac{\partial V_1(z)}{\partial z} = (R_{11} + j\omega L_{11})I_1(z) - j\omega L_{12} I_2(z), \tag{13}$$

$$-\frac{\partial V_2(z)}{\partial z} = (R_{22} + j\omega L_{22})I_2(z) + j\omega L_{12} I_2(z). \tag{14}$$

Rewriting the above equations in matrix form, we obtain:

$$-\frac{\partial}{\partial z}\overline{\mathbf{V}} = \overline{\overline{\mathbf{Z}}}\overline{\mathbf{I}}, \tag{15}$$

where

$$\overline{\overline{\mathbf{Z}}} = \begin{bmatrix} Z_{11} & Z_{12} \\ Z_{12} & Z_{22} \end{bmatrix} = \begin{bmatrix} R_{11} + j\omega L_{11} & -j\omega L_{12} \\ j\omega L_{12} & R_{22} + j\omega L_{22} \end{bmatrix} \tag{16}$$

or

$$\overline{\overline{\mathbf{Z}}} = \overline{\overline{\mathbf{R}}} + j\omega\overline{\overline{\mathbf{L}}}\,, \tag{17}$$

where the distributed resistance and inductance matrices are given by

$$\overline{\overline{\mathbf{R}}} = \begin{bmatrix} R_{11} & 0 \\ 0 & R_{22} \end{bmatrix} \text{ and } \overline{\overline{\mathbf{L}}} = \begin{bmatrix} L_{11} & -L_{12} \\ L_{12} & L_{22} \end{bmatrix}. \tag{18}$$

The elements of $\overline{\overline{\mathbf{R}}}, \overline{\overline{\mathbf{L}}}, \overline{\overline{\mathbf{C}}}$, and $\overline{\overline{\mathbf{G}}}$ may be frequency dependent, which is important in order to model more realistic cables. For didacticism, in the formula developments it was considered two parallel, coupled lines. However the expansion of the model for more parallel lines is direct, just by increasing conveniently the order of the $\overline{\overline{\mathbf{R}}}, \overline{\overline{\mathbf{L}}}, \overline{\overline{\mathbf{C}}}$, and $\overline{\overline{\mathbf{G}}}$ matrices.

From (9), by inverting the impedance matrix and performing the spatial derivative, we obtain

$$-\overline{\overline{\mathbf{Z}}}^{-1}\frac{\partial^2}{\partial z^2}\overline{\mathbf{V}} - \frac{\partial}{\partial z}\overline{\overline{\mathbf{Z}}}^{-1}\frac{\partial}{\partial z}\overline{\mathbf{V}} = \frac{\partial}{\partial z}\overline{\mathbf{I}}. \tag{19}$$

By using (9), we can rewrite (19) as

$$\frac{\partial^2}{\partial z^2}\overline{\mathbf{V}} + \overline{\overline{\mathbf{Z}}}\frac{\partial}{\partial z}\overline{\overline{\mathbf{Z}}}^{-1}\frac{\partial}{\partial z}\overline{\mathbf{V}} - \overline{\overline{\boldsymbol{\gamma}}}^2\overline{\mathbf{V}} = 0, \tag{20}$$

where $\overline{\overline{\boldsymbol{\gamma}}}^2 = \overline{\overline{\mathbf{Z}}}\,\overline{\overline{\mathbf{Y}}}$.

By neglecting the influence of localized cable discontinuities, we obtain

$$\frac{\partial^2}{\partial z^2}\overline{\mathbf{V}} - \overline{\overline{\boldsymbol{\gamma}}}^2\overline{\mathbf{V}} = 0. \tag{21}$$

The transmission matrix can be written in terms of the propagation constant $\overline{\overline{\gamma}}$ and the section length *l*, as

$$\overline{\overline{\mathbf{T}}}_{(4\times4)} = \begin{bmatrix} \overline{\overline{\mathbf{A}}}_T & \overline{\overline{\mathbf{B}}}_T \\ \overline{\overline{\mathbf{C}}}_T & \overline{\overline{\mathbf{D}}}_T \end{bmatrix} = \begin{bmatrix} \cosh(\overline{\overline{\boldsymbol{\gamma}}}l) & \overline{\overline{\mathbf{Z}}}_0 \sinh(\overline{\overline{\boldsymbol{\gamma}}}l) \\ \overline{\overline{\mathbf{Z}}}_0^{-1}\sinh(\overline{\overline{\boldsymbol{\gamma}}}l) & \cosh(\overline{\overline{\boldsymbol{\gamma}}}l) \end{bmatrix}, \tag{22}$$

where $\overline{\overline{\mathbf{Z}}}_0 = \sqrt{\overline{\overline{\mathbf{Y}}}^{-1}\overline{\overline{\mathbf{Z}}}}$.

The Transmission Matrix $\overline{\overline{\mathbf{T}}}$ in (22) describes a multiconductor section of length *l*. If *N* different sections are put together in cascade, the resulting transmission matrix is obtained by taking the product of the transmission matrices that represents each multiconductor section, considering their respective order:

$$\overline{\overline{\mathbf{T}}} = \begin{bmatrix} \overline{\overline{\mathbf{A}}}_T & \overline{\overline{\mathbf{B}}}_T \\ \overline{\overline{\mathbf{C}}}_T & \overline{\overline{\mathbf{D}}}_T \end{bmatrix} = \overline{\overline{\mathbf{T}}}_1\overline{\overline{\mathbf{T}}}_2\overline{\overline{\mathbf{T}}}_3 \ldots \overline{\overline{\mathbf{T}}}_N\overline{\overline{\mathbf{T}}}_{Load},$$

where $\overline{\overline{\mathbf{T}}}_1, \overline{\overline{\mathbf{T}}}_2, \overline{\overline{\mathbf{T}}}_3, \ldots, \overline{\overline{\mathbf{T}}}_N$ are obtained for each serial section from (22) and the transmission matrix $\overline{\overline{\mathbf{T}}}_{Load}$, assigned to the load impedance matrix $\overline{\overline{\mathbf{Z}}}_L$, is given by

$$\overline{\overline{\mathbf{T}}}_{Load(4\times4)} = \begin{bmatrix} \overline{\overline{\mathbf{I}}}_{(2\times2)} & \overline{\overline{\mathbf{0}}}_{(2\times2)} \\ \overline{\overline{\mathbf{Z}}}_L^{-1} & \overline{\overline{\mathbf{I}}}_{(2\times2)} \end{bmatrix},$$

where

$$\overline{\overline{\mathbf{I}}}_{(2\times2)} = \begin{bmatrix} 1 & 0 \\ 0 & 1 \end{bmatrix}, \quad \overline{\overline{\mathbf{0}}}_{(2\times2)} = \begin{bmatrix} 0 & 0 \\ 0 & 0 \end{bmatrix} \text{ and } \overline{\overline{\mathbf{Z}}}_L = \begin{bmatrix} R_{1B} & 0 \\ 0 & R_{2B} \end{bmatrix}.$$

The matricial forms of the transfer function and scattering matrices were adapted from their scalar forms. The scalar representations can be obtained in textbooks such as [7].

The transfer function matrix was computed by:

$$\overline{\overline{\mathbf{H}}} = \overline{\overline{\mathbf{A}}}_T^{-1}. \tag{23}$$

The scattering matrix is obtained from:

$$\overline{\overline{\mathbf{S}}} = (\overline{\overline{\mathbf{Z}}}_{in} + \overline{\overline{\mathbf{Z}}}_G)^{-1}(\overline{\overline{\mathbf{Z}}}_{in} - \overline{\overline{\mathbf{Z}}}_G),$$

where $\overline{\overline{\mathbf{Z}}}_{in} = \overline{\overline{\mathbf{C}}}_T^{-1}\overline{\overline{\mathbf{A}}}_T$.

Therefore,

$$\overline{\overline{\mathbf{S}}} = (\overline{\overline{\mathbf{C}}}_T^{-1}\overline{\overline{\mathbf{A}}}_T + \overline{\overline{\mathbf{Z}}}_G)^{-1}(\overline{\overline{\mathbf{C}}}_T^{-1}\overline{\overline{\mathbf{A}}}_T - \overline{\overline{\mathbf{Z}}}_G), \tag{24}$$

where $\overline{\overline{\mathbf{Z}}}_G$ is the generator impedance matrix, at the central office.

The FEXT transfer functions are obtained from the off-diagonal elements of $\overline{\overline{\mathbf{H}}}$ whereas NEXT transfer functions are obtained from the off-diagonal elements of $\overline{\overline{\mathbf{S}}}$.

III. Results

To validate the proposed approach, the loop scenario chosen for simulation consists of two parallel transmission-lines composed by polyethylene (PE) 0.63 mm diameter cables. The diagonal elements of the $\overline{\overline{\mathbf{R}}}$ and $\overline{\overline{\mathbf{L}}}$ matrices are frequency dependent and their values over frequency were obtained from [6] and their formulae are shown in Appendix I. For this cable, the distributed capacitance of each line is

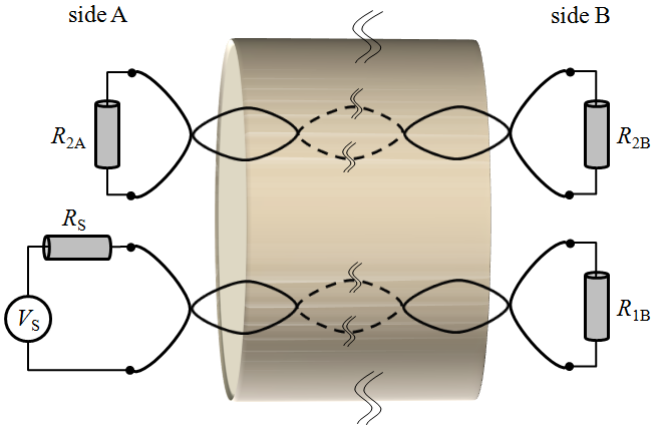

Fig. 2. Telephone loop considered for FDTD simulation.

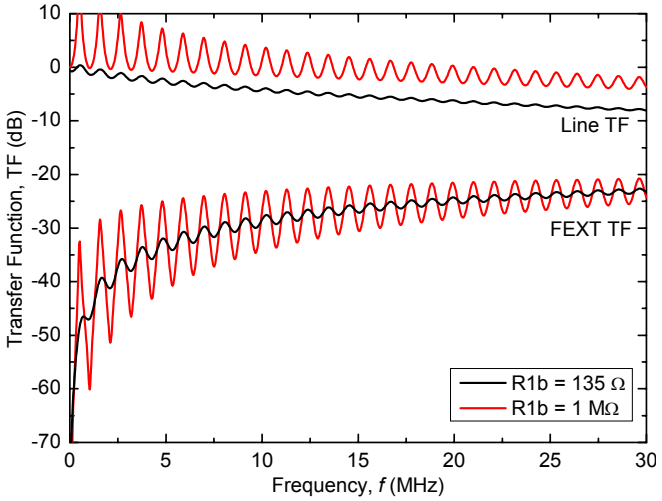

Fig. 3. Transfer function of the transmitting line and FEXT coupling into the other line.

C_{11} = C_{22} = 45 pF/m in (12). The distributed conductance G_{11} and G_{22} are negligible. The length of both lines is l = 100 m.

In practice, the off-diagonal terms values of the electrical parameters matrices are a very small fraction of the diagonal ones, depending on the distance between pairs. In the simulations, it was assumed that C_{12}=0.09 pF/m, L_{12}=1.0 nH/m ang G_{12} = 0. The values of termination impedances are $R_S = R_{2A} = R_{2B}$ = 135Ω and R_{1B} is assumed variable. The direct and FEXT transfer functions are shown in Fig 3, and the NEXT transfer function is shown in Fig 4. The graphs illustrate that, for short length binders, load mismatches at the transmitting line cause oscillations at FEXT transfer function and also enhances significantly NEXT coupling into neighboring pairs, which impairs their data transmission.

The phase of FEXT and NEXT, compared with the phase of the line transfer function, are shown at Figs. 5 and 6, respectively. The variable load impedance is R_{1B} = 135Ω. It can be noted a constant delay on FEXT phase, probably due the combined influence of the inductive and capacitive cross-coupling between lines. The phase variation of NEXT (Fig. 6) is two times the phase variation of the line transfer function, which suggests that, for this line configuration, most of NEXT interference is caused by reflections due impedance mismatches at the right end of the lines, and thus the signal propagates back again over the binder length, until it arrives at R_{2A} terminal, which characterizes the NEXT noise.

Finally, in order to check the method, a particular case was simulated and compared with the finite-difference time-domain (FDTD) [10]. Since the developed FDTD method does not considers dispersive parameters, R_{11}, R_{22}, L_{11} and L_{22} were assumed constant with frequency for this test. The modified parameters are $R_{11} = R_{22}$ = 1.0734 Ω/m, $L_{11} = L_{22}$ = 489.11 nH/m, and all source and load impedances were set to 100 Ω. The line transfer function and crosstalk (FEXT and NEXT) transfer functions obtained with both methods are shown in Fig. 7. The concordance between the transmission matrix method results and those obtained via FDTD method was very satisfactory.

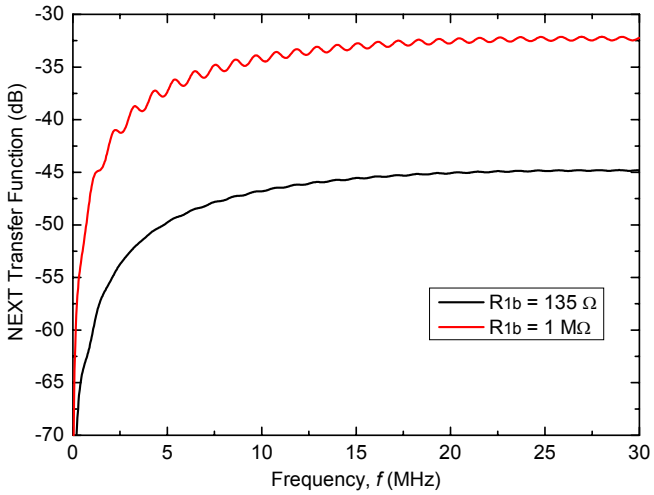

Fig. 4. NEXT transfer function.

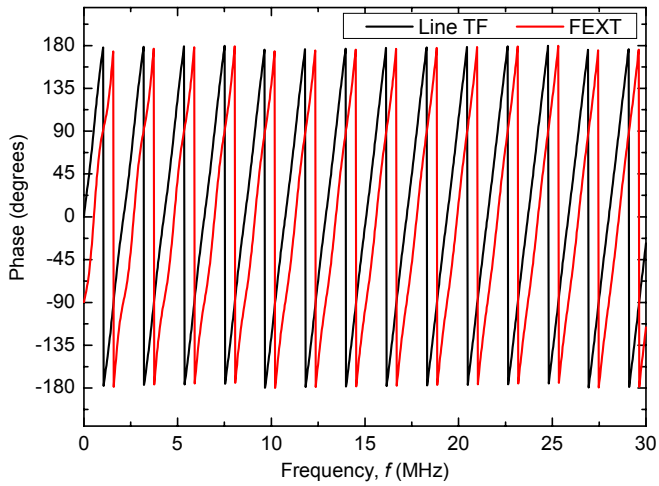

Fig. 5. Phase of FEXT, compared with the phase of line transfer function.

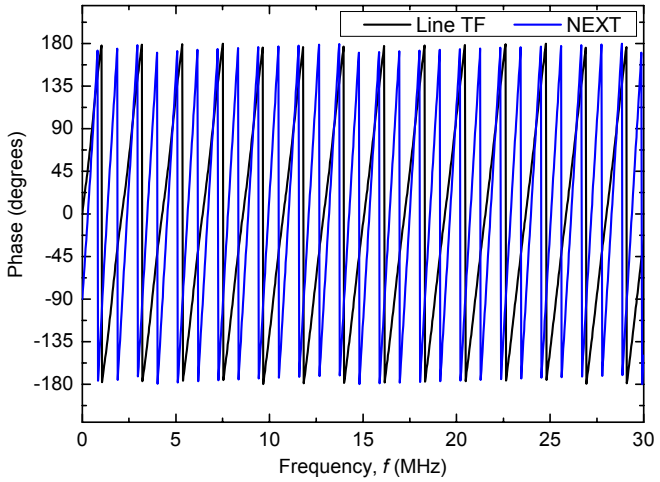

Fig. 6. Phase of NEXT, compared with the phase of line transfer function.

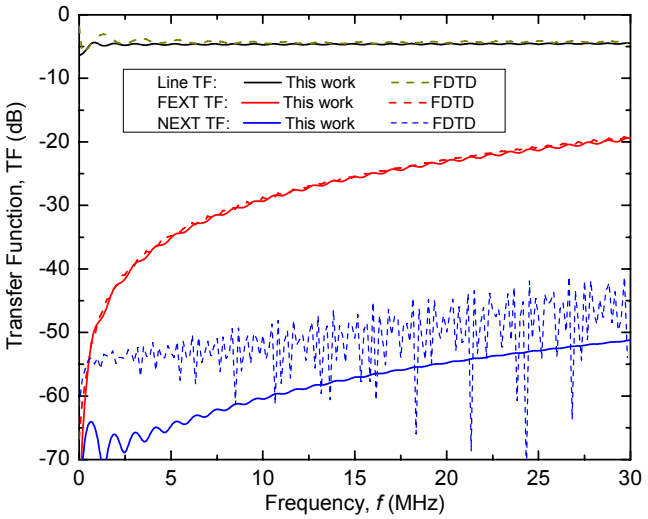

Fig. 7. A comparison between the transmission matrix method (this work) and the FDTD method [10].

IV. Conclusion

A multiconductor approach with differential setup was developed to simulate broadband signal transmission over telephone binders. Results show that crosstalk interference may be severe for short loops and higher frequencies. NEXT noise level is also increased when load mismatches are present. The exposed technique is suitable to estimate channel capacity, considering mutual interference between two or more pairs.

Appendix I

The frequency dependence of the distributed resistance and capacitance for polyethylene (PE) cables are characterized below [6].

$$R = \left(r_{oc}^{\ 4} + a_c f^2\right)^{\frac{1}{4}}, \tag{25}$$

$$L = \frac{L_0 + L_8 x_b}{1 + x_b}, \tag{26}$$

where $x_b = (f / f_m)^b$ and f is the frequency. The six coefficients for typical wire gauges are given in Table I.

TABLE I
Coefficients for Calculation of R and L

Gauge (mm)	r_{oc} (Ω/m)	a_c $\left[\frac{(\Omega/m)^4}{MHz^2}\right]$	L_0 (nH/m)	L_8 (nH/m)	fm (MHz)	b
0.32	0.4090	0.3822	0.6075	0.5	0.6090	5.269
0.4	0.2800	0.0969	0.5873	0.4260	0.7459	1.385
0.5	0.1792	0.0561	0.6746	0.5327	0.6647	1.195
0.63	0.113	0.0257	0.6994	0.4772	0.2658	1.0956
0.9	0.0551	0.0094	0.7509	0.5205	0.1238	0.9604

References

[1] C. R. Paul and J. W. McKnight, "Prediction of crosstalk involving twisted pairs of wires —Part I: A transmission-line model for twisted-wire pairs," IEEE Trans. Electromagn. Compat., vol. 21, pp.92–105, May 1979.

[2] C. R. Paul and J. W. McKnight, "Prediction of crosstalk involving twisted pairs of wires —Part II: A simplified low-frequency prediction model," IEEE Trans. Electromagn. Compat., vol. 21, pp. 105–114, May 1979.

[3] C. R. Paul, Introduction to Electromagnetic Compatibility. Wiley-Interscience, 1992, ch. 10.

[4] A. R. Djordjevic, T. K. Sarkar, R. F. Harrington, "Time-domain response of multiconductor transmission lines", *Proc. IEEE*, vol.75, no. 6, June 1987, pp.743-764

[5] C. R. Paul, Analysis of Multiconductor Transmission lines. New York : Wiley, 1994.

[6] ITU-T Recommendation G.996.1, "Transmission Systems and Media – Test Procedures for Digital Subscriber Line (DSL) Transceivers", 1999.

[7] D. M. Pozar, Microwave Engineering, 2nd ed. New York:Wiley, 1998.

[8] T. Magesacher et al., "Verification of multipair copper-cable model by measurements," IEEE Trans. Instr. Meas., vol. 56, pp. 1883–1886, Oct 2007.

[9] Cioffi T. Starr, J. M. Cioffi, and P. J. Silverman, Understanding Digital Subscriber Line Technology. Englewood Cliffs, NJ: Prentice-Hall, 1999.

[10] L. D. S. Alcantara, J. C. W. Albuquerque Costa, B. Dortschy and A. Klautau, "Crosstalk Analysis in Transmission Lines with Differential Excitation Using FDTD," *in Proc. MOMAG Conf.*, Florianópolis, Brazil, 2008, pp. 484–488.